Heliyon 10 (2024) e34891

Contents lists available at ScienceDirect

Heliyon

journal homepage: www.cell.com/heliyon

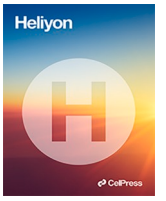

Research article

Study on the sliding mechanism of the external dump slope in the open-pit mine with wind-blown sand base

Hongze Zhao [a,b,*], Yan Lu [a], Binde Qin [c], Qiang Hao [d], Yu Sun [e]

[a] School of Energy and Mining Engineering, China University of Mining and Technology (Beijing), Beijing, 100083, China
[b] State Key Laboratory of Deep Rock Mechanics and Underground Engineering, China University of Mining and Technology (Beijing), Beijing, 100083, China
[c] Gas Research Branch, China Coal Technology and Engineering Group Chongqing Research Institute, Chongqing, 400037, China
[d] Huaneng Coal Technology Research Co., Ltd., Beijing, 100070, China
[e] CHN Energy Coal Safety Supervision Center, Ordos, 017010, China

ARTICLE INFO

Keywords:
Waste dump
Wind-blown sand
Failure mode
Similarity simulation
Numerical simulation

ABSTRACT

Wind-blow sand (WBS) is widely distributed in the "Desert Gobi" region. This study is aimed at exploring the mechanism of how different thicknesses of the WBS layer influence the slope movement of external dumps in open-pit mines. To achieve this aim, the slope of the external dump in the open-pit mining area of Panel 3 in Daliuta Coal Mine was taken as the research object. First, similar simulation experiments were performed for investigating the failure modes and deformation characteristics of the external dump slopes under three geo-morphological conditions: loess base, 10-m-thick WBS base, and 20-m-thick WBS base, respectively. The following results were obtained from the experiments. For the slope with a loess base, its failure is mainly caused by circular sliding from the dump to the interior of the loess layer. For the slope with a 10-m-thick WBS base, the sliding mode involves circular sliding from the dump area to the interior of the WBS layer, linear sliding along the WBS base, and shearing along the foot of the dump area. For the slope with a 20-m-thick WBS base, the sliding mode is circular sliding from the dump area to the interior of the WBS layer. Besides, the sliding area of the dump slope expands as the WBS layer thickens. Furthermore, the results of similar simulation experiments were verified by the finite difference software FLAC^{3D} based on the strength reduction method, and an equation of relationship between the safety factor of the dump slope with a WBS base and the thickness of the WBS layer was derived.

1. Introduction

In open-pit mining, slopes are faced with considerable safety hazard. The stability of such slopes, which affects the safe production of the entire open-pit mine [1,2], is subject to multiple factors including geological conditions, natural phenomena, and human activities. Hence, its evaluation requires comprehensive consideration.

A variety of studies have been conducted on the stability of open-pit slopes, and the yielded research results are of guiding significance for evaluating and improving the stability of open-pit slopes. Based on key block theory analysis, Zerradi et al. proposed a method to select a suitable slope for different discontinuous rock masses in an open-pit mine in Morocco. The results show that the

* Corresponding author. School of Energy and Mining Engineering, China University of Mining and Technology (Beijing), Beijing, 100083, China.
E-mail address: hzzhao78@163.com (H. Zhao).

https://doi.org/10.1016/j.heliyon.2024.e34891
Received 17 February 2024; Received in revised form 26 June 2024; Accepted 18 July 2024
Available online 19 July 2024

maximum safe slope angle of the research platform lies in the range of 63°–73°, which is closer to on-site conditions than 58°–78° that is previously used in the mine. This method can be used to design or evaluate the slope stability of open pit dumps [3]. By combining numerical simulation with probability analysis, Sdvyzhkova et al. revealed the probability of surrounding rock stability loss in open pit mines and the situation where the strength reduction coefficient falls to below the standard level at each stage of orebody mining. The research results contribute to formulating reinforcement measures in areas where the strength reduction factor is below the standard value and determining the dependence of the variation of the safety factor of each mining layer rock, and can serve as a basis for the subsequent optimization of the contour line of open-pit subdivision [4]. Based on the basic principles and methods of fuzzy mathematics and GIS, Sun et al. established a fuzzy comprehensive evaluation and analysis model for slope stability, and determined the classification index for slope stability [5].

To better control the stability of open-pit slopes, it is necessary to investigate the key factors affecting the slope. Fan et al. found that the weak inter-layer, as a typical geological structure, exerts a key impact on slope stability. The slope safety factor grows with the increase in the buried depth of the weak inter-layer, and it tends to stabilize when the buried depth reaches a certain value. In addition, as the angle of the weak inter-layer rises, the failure mechanism shows progressive changes of inter-layer dislocation, creeping along the bedding, and shear sliding along the weak structural plane [6]. With an open-pit coal mine in Poland as the research object, Nguyen et al. conducted a numerical simulation on the dump slope under rainfall conditions, concluding that the slope tends to be loose and stable under high rainfall intensity and short rainfall duration. On this basis, they proposed a method of soil napping combined with steel mesh to strengthen the slope [7].

Dumps store the waste of open pits, which often witness landslide accidents of open pits. Therefore, study on the sliding mechanism of open-pit dump slopes is of prime importance. Scholars have extensively studied the failure mode and deformation characteristics of open-pit dump slopes, and made contributions to grasping the sliding mechanism of open-pit dump slopes and preventing the landslide of dumps. Wang et al. focused on the dump slope outside JiaMa Copper Mine in Xizang, China, and investigated the failure mode of a steeply inclined dump with a weak base through bottom friction similar simulation experiments and numerical simulations using Geostudio software modules SIGMA/W and SLOPE/W [8]. With the aid of PFC software, Zhang et al. simulated the slope of an open pit dump in Pingshuodong Coal Mine, China, and found that the potential landslide mode of the dump is circular landslide occurring inside the upper dump [9]. According to the geological characteristics of Harwusu Open-pit Mine, Fu et al. proposed and explained seven potential landslide modes in the mine dump, and finally reached the conclusion that the failure mode of the dump is sliding along the inner part of the dump itself and sliding along the base type of the waste [10]. Based on the strength reduction method, Zhang et al. analyzed the downdip weak mudstone-base dump in Shunxing Open-pit Mine, China. The analysis unveils that the failure mode of the dump is the bedding failure along the surface of the upper waste layer to the cutting layer of the base surface, and that the failure mechanism is tensile fracturing and shearing [11]. With a dump in Nigeria as the research object, Igwe et al. conducted geo-technical tests on various soil samples in the mine, and analyzed the stability of the dump slope by numerical simulation. It is concluded that the failure modes are shallow failure, polygonal failure, and deep circular landslide in few cases [12]. Jayaweera et al. focused on the dump collapse of an open pit mine in Sri Lanka and identified the failure mode as deep (rotating) slope failure [13].

Wind-blown sand (WBS), characterized by small particle size, low surface activity, and loose texture, is widely distributed in deserts, Gobi, and other areas globally. WBS with poor gradation and no cohesiveness finds it difficult to take shape, and its shear resistance is poor even after it takes shapes. Scholars have carried out researches on the characteristics of WBS through engineering applications. Li et al. tested and analyzed the physical and mechanical properties of WBS and loess-mixed fill. The results showed that WBS and loess are similar with respect to main composition and chemical composition, both belonging to inorganic soil, but they differ notably in mineral proportion and micro-structure, and the particle density of WBS is higher [14]. Jia et al. conducted laboratory tests and theoretical calculation on the physical-mechanical properties and compaction mechanism of WBS. Based on the obtained results, they pointed out how to use WBS as roadbed materials, and disclosed that water content does not have an obvious impact on the compressibility and shear strength of WBS and WBS can be compacted under both dry and wet conditions [15]. By mixing WBS with other materials as the filling body to fill coal mines, Wang et al. obtained the characteristics of WBS materials at different times and ratios, and found that the addition of fiber can improve the brittleness of WBS filling materials [16].

When a dump is located above a WBS layer, the WBS layer becomes one of the main factors affecting the stability of the dump slope. Compared with general slopes, the slope of a WBS base dump is of unique sliding mechanisms, so the research on it is of theoretical and practical engineering significance.

The open-pit mining area of Panel 3 in Daliuta Coal Mine, China, is in the transition zone from the Loess Plateau to the WBS area of Ordos Plateau. Due to the geological influences, the surface is covered with a thick WBS layer. The layer is of low shear strength and softens easily when exposed to water, thus seriously affecting dump stability. In this study, with the dump outside Panel 3 taken as the research object, the slope sliding mechanism of the WBS base dump was explored, and the failure modes and deformation characteristics of the WBS base slope were discussed through similar simulation experiments. Furthermore, the results were verified by means of numerical simulation. Finally, an equation of relationship between the thickness of WBS and the safety factor of the slope is obtained. The research results are expected to provide reference for mining areas in the Gobi desert and areas prone to sand accumulation.

2. Study area

2.1. Mining area profile

The open-pit mining area of Panel 3 in Daliuta Coal Mine, located in Daliuta Town, Fugu County, Yulin City, Shaanxi Province,

China, is facilitated with convenient transportation and covers a mining area of about 9.955 km^2. The mining area is rich in coal resources, boasting coal reserves of over 30 million tons. The designed annual output is 2.0 Mt/a, and the service life of the mine is calculated as 16.9 a. The main mining coal seam is the 2-2 coal seam which extends into the 2-2 upper coal seam and the 2-2 coal seam inside the open-pit mining area of Panel 3. The coal seam is 3.74 m thick on average and has sound coal quality and favorable mining conditions. The open-pit mining area is mined intermittently, and the dumping operation is completed by dump trucks. The traffic location of Panel 3 is depicted in Fig. 1.

2.2. Geological features

The open-pit mining area of Panel 3 is in Shenmu Mining Area, Yulin City, Shaanxi Province, China. From old to new, the mining area strata are the Triassic Yongping Formation (T3y), the Lower Jurassic Fuxian Formation (J1f), the Middle and Lower Yan'an Formation (J1-2y), the Middle Zhiluo Formation (J2Z), the Anding Formation (J2a), the Tertiary system (R), and the Quaternary system (Q). The mining area is of gentle terrain with simple structure. Affected by the Mu Us Desert, most of the mining area surface is covered by loose WBS whose thickness varies remarkably. To be specific, loose WBS is thicker (40–70 m) in the southeast and north of the mining area, while it is thinner (32.9 m on average) in the east and west.

2.3. Mechanical parameters of rock and soil

The physical and mechanical parameters of rock and soil mass affect the deformation characteristics and failure modes of slopes. With reference to the results of indoor physical and mechanical experiments on rock and soil mass and the geological exploration data of the open-pit mining area of Panel 3, a physical and mechanical index system for this study was determined comprehensively (Table 1).

3. Similar simulation experiment

3.1. Slope failure mechanism

Slope deformation is determined by its own elastic properties and shear properties. Whether slope instability occurs is mainly determined by its own shear strength [17]. When the load on the slope exceeds its own shear strength, a plastic zone will be formed in the slope. When plastic zones connect to penetrate the slope, the slope will fail. Slope deformation consists of elastic deformation and plastic deformation:

$$\varepsilon = \varepsilon_1 + \varepsilon_2$$

where ε, ε_1, and ε_2 are total strain, elastic strain, and plastic strain, respectively.

As WBS belongs to a weak rock stratum characterized by low shear strength, the slope stability is correlated to the thickness of WBS to a great extent. In the case of a thin WBS layer, the slope failure mode is dump sliding. However, in the case of a thick WBS layer,

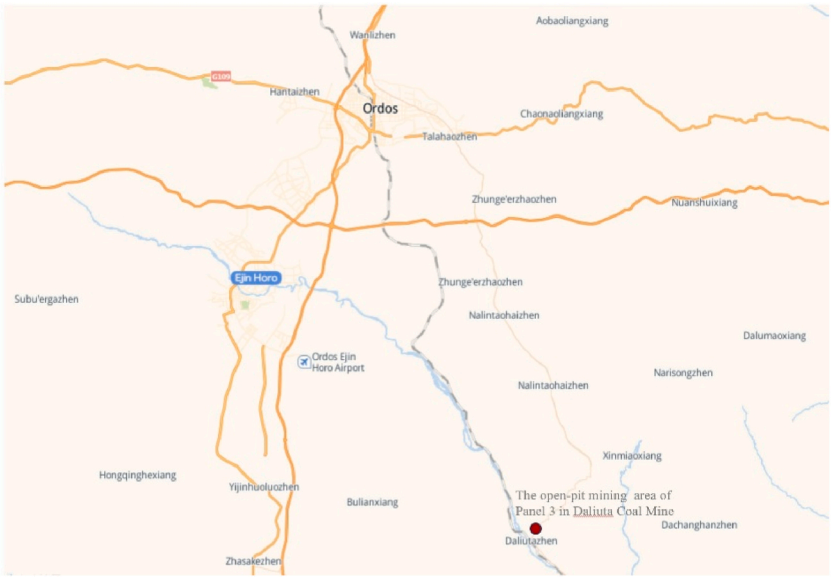

Fig. 1. Traffic location of Panel 3 in Daliuta Coal Mine.

Table 1
Physical and mechanical parameters of rock and soil.

Stratigraphic characteristics	Density/g/cm^3	Elastic modulus/MPa	Poisson's ratio	Cohesion/Kpa	Angle of internal friction/°
Waste	1.88	105	0.4	40	25.6
WBS	1.6	286	0.25	0	22
Loess	1.86	192	0.3	15	26
Bedrock	2.445	7520	0.204	3630	38.97

fractures gradually emerge inside the dump slope with the increase in load. The strong fluidity of WBS leads to the settlement of the underlying WBS, resulting in the pulling and fracturing of the dump. Under this condition, the failure mode of the slope is the circular sliding from the dump to the inside of WBS as well as the pulling and fracturing of the dump caused by the underlying WBS. The damage of the dump slope is illustrated in Fig. 2.

3.2. Experimental design

To explore the deformation characteristics and failure modes of the external dump slopes with different WBS thicknesses, the section of the external dump in the open-pit mining area of Panel 3 in Daliuta Coal Mine was selected for constructing three external dump slope models with WBS base thicknesses of 0 m, 10 m and 20 m, respectively. The failure modes of the three models under loading were recorded, and the displacement variations were monitored.

The similar simulation experimental models were set up inside a model box [18] that was 1.6 m long, 0.8 m wide, and 1 m high (see Fig. 3). The four sides of the model box were surrounded by 1-cm-thick transparent glass plates. The failure states of the slope models and the displacement changes at monitoring points could be observed through the front and rear glass plates. The left side of the model box was a steel baffle, and a wedge block was set between the baffle and the rear glass plate. The steel plate and the wedge block could mitigate the impact on the rear glass plate to a certain extent if the models collapsed during the box elevation along the left side. The right side of the model box was a hydraulic support column, which was connected to the steel base at the bottom. The model box could be rotated and lifted to a certain angle along the left side by the hydraulic support column, simulating a sloping base for dump [19].

In the box-type similar simulation experiment, some external conditions were required to induce landslide in the slope models. Specifically, a pressure plate needed to be placed on the model top, and a load block needed to be laid on the pressure plate to apply load and achieve model failure. In the hope of ensuring uniform loading on the model top, the model top should be horizontal and smooth. Additionally, the pressure plate should be made of materials with sufficient stiffness. The region where the model is subject to loading is presented in Fig. 4. To prevent the model from experiencing rib spalling or collapse under the compressive state of the top during experiment, boundary constraints needed to be set for the model during loading. Specifically, the out sides of the model were blocked, so as to ensure that the entire model only had a free surface at the top and merely experienced horizontal and vertical displacements.

In this experiment, monitoring points were arranged on the model sides for the purpose of grasping the deformation characteristics of the slope and monitoring changes in slope displacement. Reflective markers (size 2 cm × 2 cm) were placed at these monitoring points. To be specific, they were inserted at appropriate positions on the model sides with large-headed pins, and the deformation characteristics of the model could be obtained by monitoring their displacement.

3.3. Similarity experimental model

The similarity ratio requires comprehensive consideration of the engineering prototype and test conditions. According to the sizes of the model box and the engineering prototype, the geometric similarity constant $C_l = 100$, the density similarity constant $C_\rho = 1.2$, and the stress similarity ratio $C_\sigma = 120$ by calculation.

In similar simulation experiments, similar materials are crucial for the experimental accuracy. Considering the prototype characteristics in this experiment, the filling material is sand, and the bonding materials include white cement and gypsum [20].

Moreover, the physical and mechanical parameters of the same similar material at different material ratios can also vary

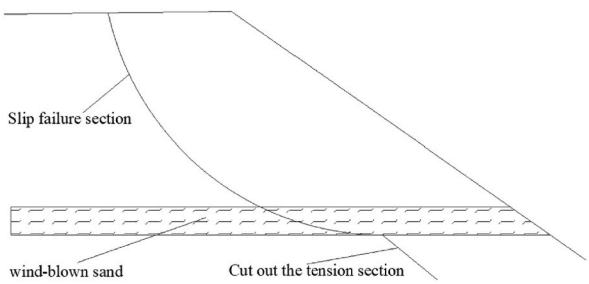

Fig. 2. Damage diagram.

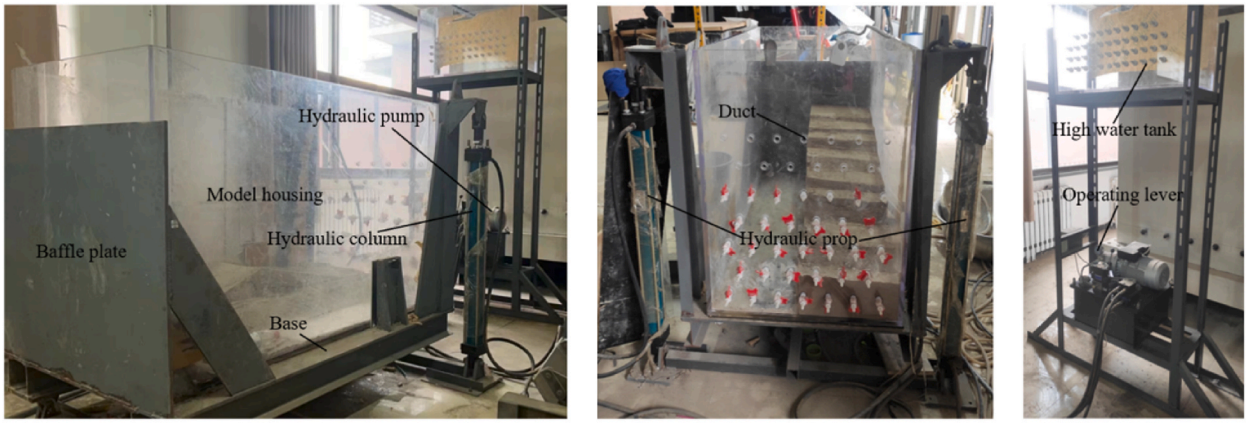

Fig. 3. Diagram of model box.

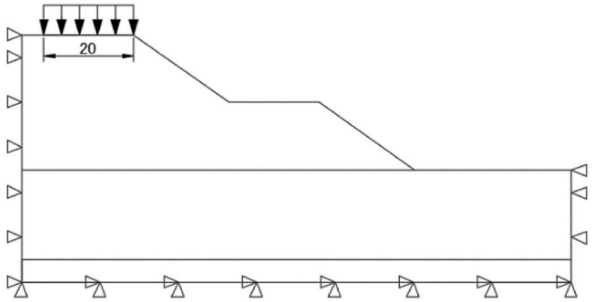

Fig. 4. Loading area.

significantly. Based on experience and experimental data, the material ratios for this study are acquired (Table 2). With the ratios for the model materials, the similarity ratios, as well as the physical and mechanical parameters of the original rock, the mechanical parameters of the similar materials can be obtained (Table 3 [21]).

Based on the above material ratios, experimental models were established with the dump base composed of WBS and loess. The thickness of the WBS layer ranges from 0 m to 20 m, approximately 10 m on average. The average thickness of the loess layer is around 20 m. To obtain the failure modes and deformation characteristics of the dump slope under different WBS thicknesses, slopes with WBS thicknesses of 0 m, 10 m, and 20 m were established [22,23].

According to the engineering prototype, two levels of dumping benches were established in the dump model. The model widths of the first and second benches were 20 cm and 25 cm respectively, the height and slope angle of the benches being 15 cm and 35° respectively. In addition, the schematic diagram of Model A (loess layer actual thickness 20 m and WBS layer actual thickness 0 m) is exhibited in Fig. 5.

After the addition of the WBS layer, the bedrock exerts an insignificant influence on the damage and deformation of the upper dump slope. To facilitate operation, the bedrock is removed. The schematic diagram of Model B (WBS layer actual thickness 10 cm) is shown in Fig. 6. The schematic diagram of Model C (WBS layer actual thickness 20 cm) is shown in Fig. 7.

3.4. Loading and data monitoring

Upon the completion of monitoring point arrangement, the models were subject to loading, during which the deformation characteristics and failure process of the models were recorded. When the model no longer changed, that is, when the displacements at

Table 2
Model material ratios.

Category	Sand	Lime	Gypsum
Waste	9	6	4
WBS	8	5	5
Loess	8	3	7

Table 3
Mechanical parameters of similar materials.

Category	Bulk density γ/KN/m^3	Cohesion C/KPa	Angle of internal friction ϕ/°	Poisson's ratio ν
Waste	15.35	0.333	25.6	0.4
WBS	13.07	0	22	0.25
Loess layer	15.19	0.125	26	0.3

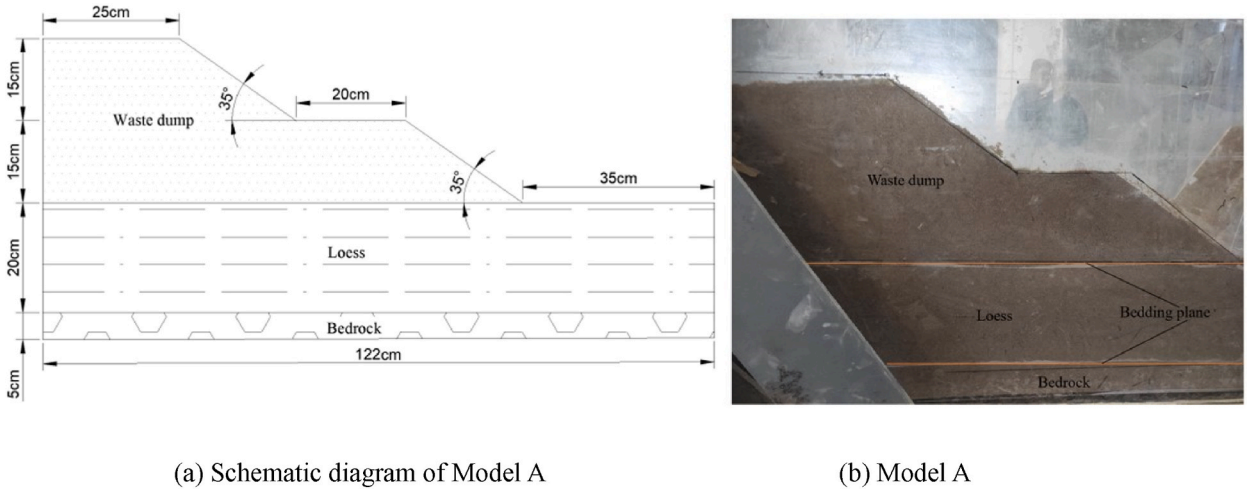

Fig. 5. Schematic diagram of Model A (WBS layer actual thickness 0 m).

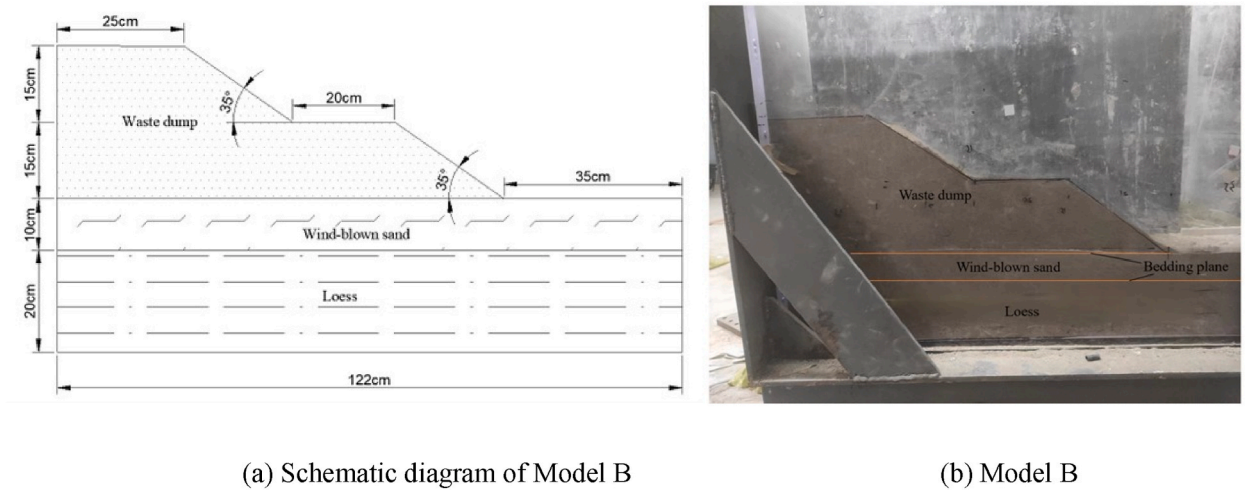

Fig. 6. Schematic diagram of Model B (WBS actual thickness 10 m).

monitoring points on the models became smaller than 0.1 mm, the deformation and failure states on the side and slope of the models were observed and recorded, and the displacements at monitoring points were recorded as well. Once this stage was completed, the next level of loading started. The above steps were repeated until the model failed completely.

Data regarding the model destruction process were collected and collated, and the displacement data at monitoring points in different loading stages were exported. Subsequently, the obtained experimental images and monitoring point displacement data were analyzed to find the failure modes and deformation patterns of the dump slopes under different thicknesses of the WBS layer.

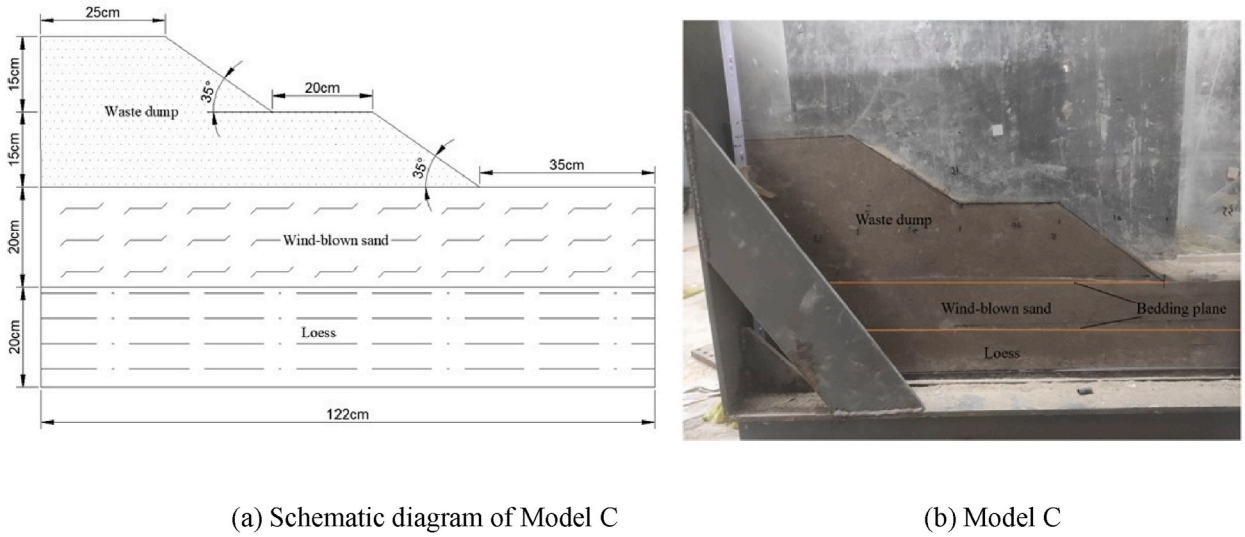

Fig. 7. Schematic diagram of Model C (WBS layer actual thickness 20 m).

4. Experimental results and analysis

4.1. Failure characteristics of models

Fig. 8 shows the failure process of Model A. As the test proceeds, under the action of berm loading on the upper part of the second bench, oblique cracks are formed below the top of the second bench. The reason is that under the loading of the dump upper part, shear strain occurs inside the dump, and a transverse crack is generated beneath the lower part of the second bench. Another transverse crack is formed under the formed transverse crack, and the cracks below the top of the second bench continues to develop. Correspondingly, a downward crack is formed at the contact between the waste layer and the loess layer, and an upward crack is formed below the slope of the first bench. This is because Model A experiences a certain degree of deflection towards the left empty side. In the fourth stage, two cracks are formed on the slope of the first bench of the dump as a result of stress concentration on the slope caused by the gradual development of the crack on the left side. When the crack on the upper part of the second bench is connected with the slope of the first bench, Model A fails. The failure mode is mainly circular sliding from the dump to the inside of the loess layer.

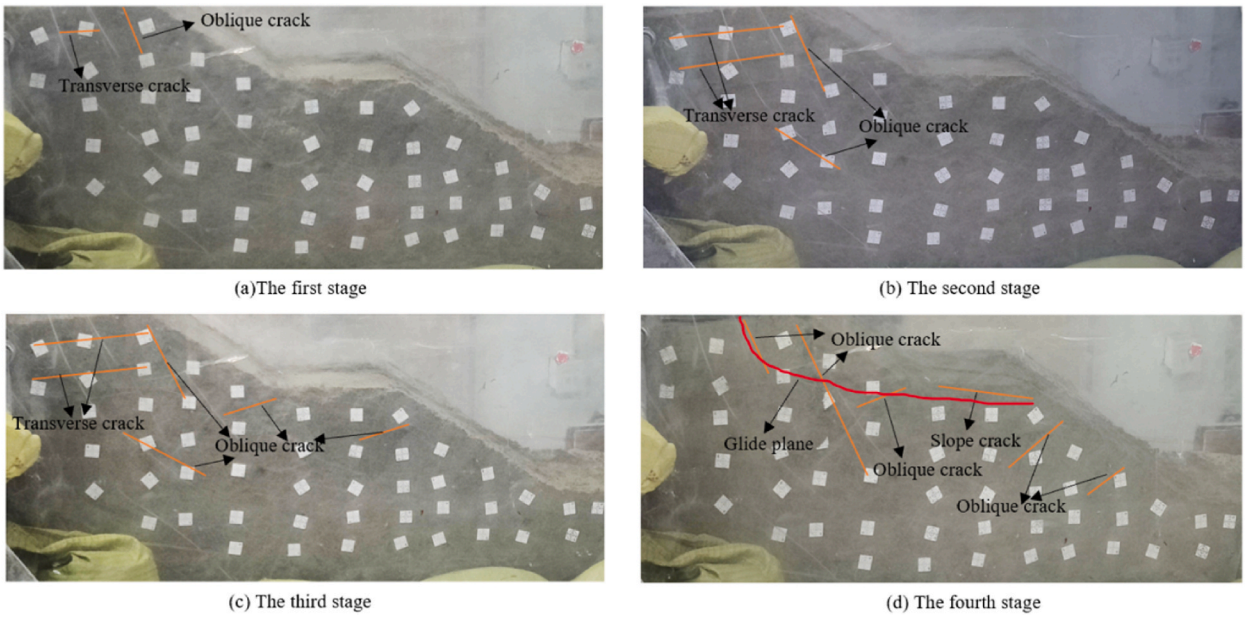

Fig. 8. Failure process of Model A.

Fig. 9 gives the failure process of Model B. It can be observed that under the loading of the second bench, a circular arc-shaped crack first appears below the berm of the second bench, which arises from the shear strain within the dump under loading. As the experiment continues, an oblique crack emerges above the circular arc-shaped crack, which is induced by shear strain within the dump due to upper loading. Meanwhile, two oblique cracks are formed below the circular arc-shaped crack, which are jointly caused by shear strain within the dump and settlement of the underlying WBS layer. As the experiment proceeds, existing cracks continue to develop and widen. Three oblique cracks appear below the second bench. One of them, being nearly vertical, mainly results from the settlement of the underlying WBS layer, and the other two oblique cracks result from shear strain generated by upper loading of the dump and settlement of the WBS layer, respectively. In the fourth stage, cracks develop and widen further, and the WBS layer is extruded under the loading of the upper berm of the dump. This is mainly attributed to the fact that the low shear strength and high fluidity of the WBS layer make it prone to extrusion under stress loading. Cracks extend downward towards the first bench of the dump. The experimental results indicate that the failure of Model B mainly belongs to internal sliding of the dump and the pulling and fracturing of the dump caused by the settlement of the underlying WBS layer, with the fracture area mainly located at the lower part of the second bench.

Fig. 10 displays the failure process of Model C. As can be seen from Fig. 10, in the initial loading state, the dump first generates an obliquely downward crack below the berm of the second bench. This phenomenon can be explained as follows: under the loading of the berm on the upper part of the second bench, shear forces are generated inside the dump, bringing about the generation of shear strain and the formation of an oblique crack. A transverse crack is formed at the lower part of the corner of the second bench, directed towards the empty side of the second bench. This crack is also induced by the shear forces produced within the dump by the upper dump loading. As the experiment continues, a transverse crack occurs below the berm on the upper part of the first bench. This is because an empty side exists at the first bench, towards which the dump splits under compression, resulting in the generation of a transverse crack. As the experiment goes on, the cracks further develop and widen continuously. Afterwards, a fracture zone is formed at the lower part of the second bench under the joint effects of shear forces acting on the dump and settlement of the underlying WBS layer. Eventually, the cracks extend into the WBS layer, indicating that the failure mode of the dump is the pulling and fracturing of the dump caused by internal sliding of the dump and settlement of the underlying WBS layer. The fracture zone of the dump is beneath the slope foot of the second bench.

4.2. *Deformation characteristics of models*

According to the displacement of monitoring points on the slope sides of the three models, corresponding horizontal displacement contour maps were plotted using ORIGIN software (Fig. 11). For the three models, the horizontal displacement contours are all approximately arc-shaped, meaning that arc-shaped sliding is their main sliding mode. However, their positions and sizes of the sliding surface differ due to their different thicknesses of the WBS layer. For Model A, a large arc-shaped sliding surface and a small one can be observed at the first and second benches, respectively. This suggests that Model A experiences arc-shaped sliding from the dump to the interior of the loess layer. In contrast, Model B has a larger sliding range but a lower sliding surface. Linear distribution is observed

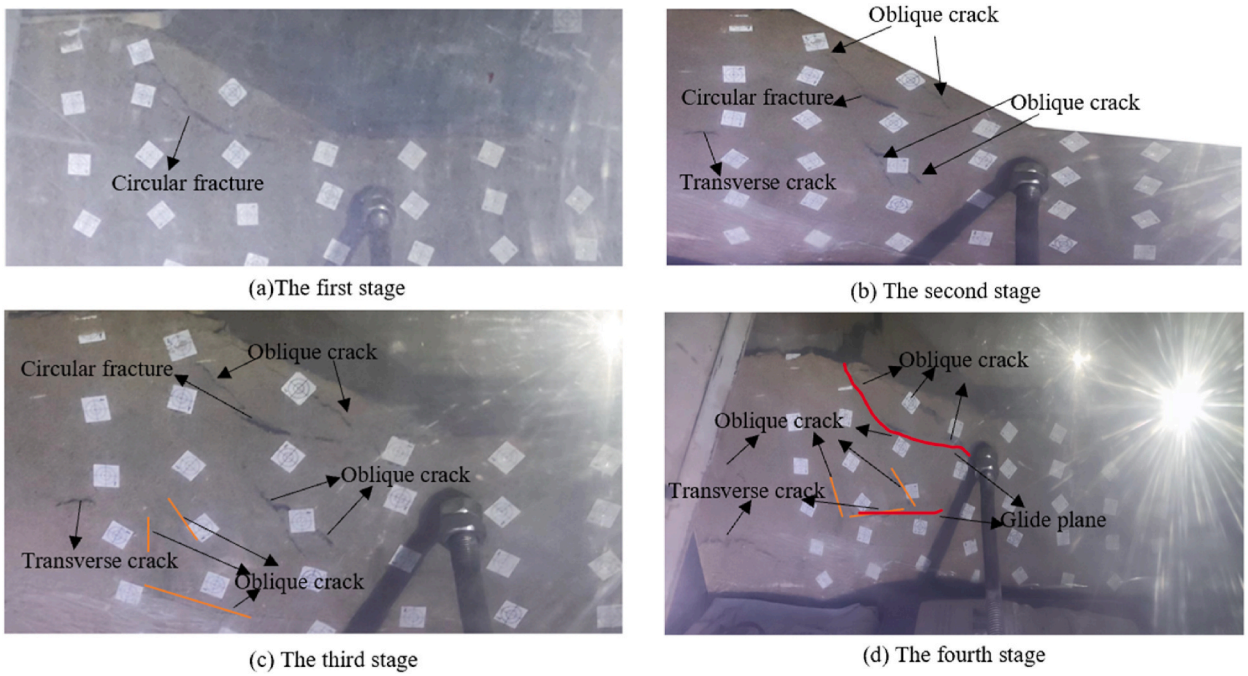

Fig. 9. Failure process of Model B.

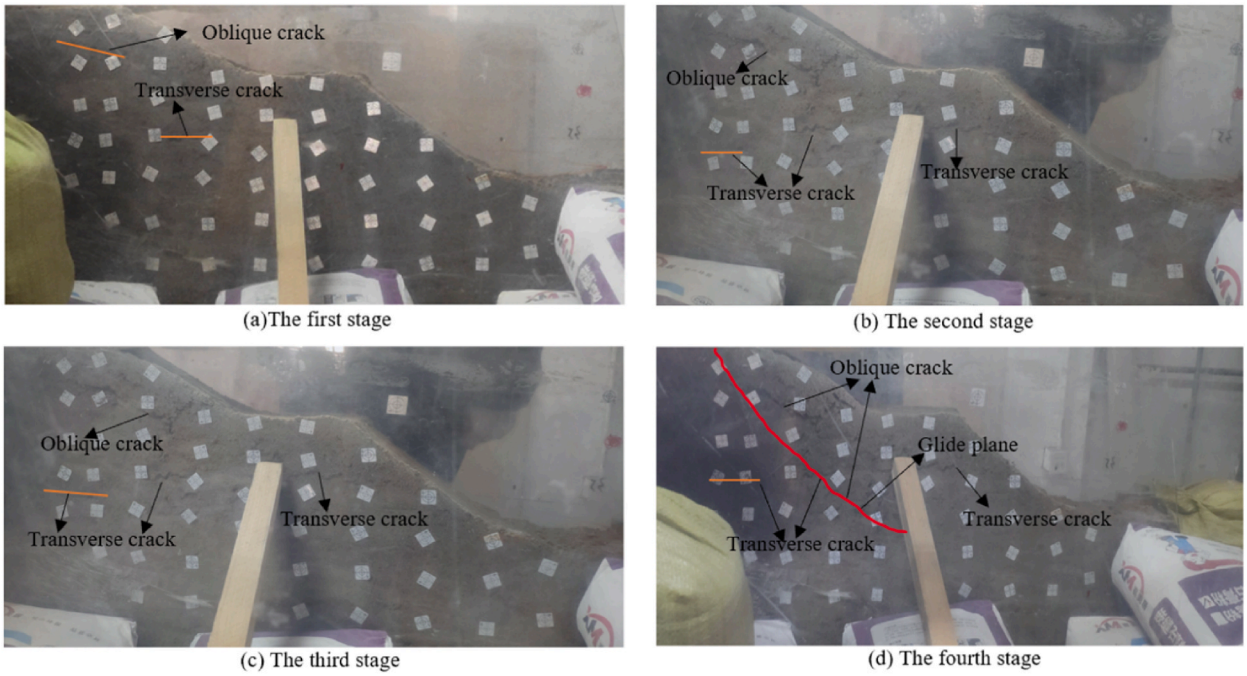

Fig. 10. Failure process of Model C.

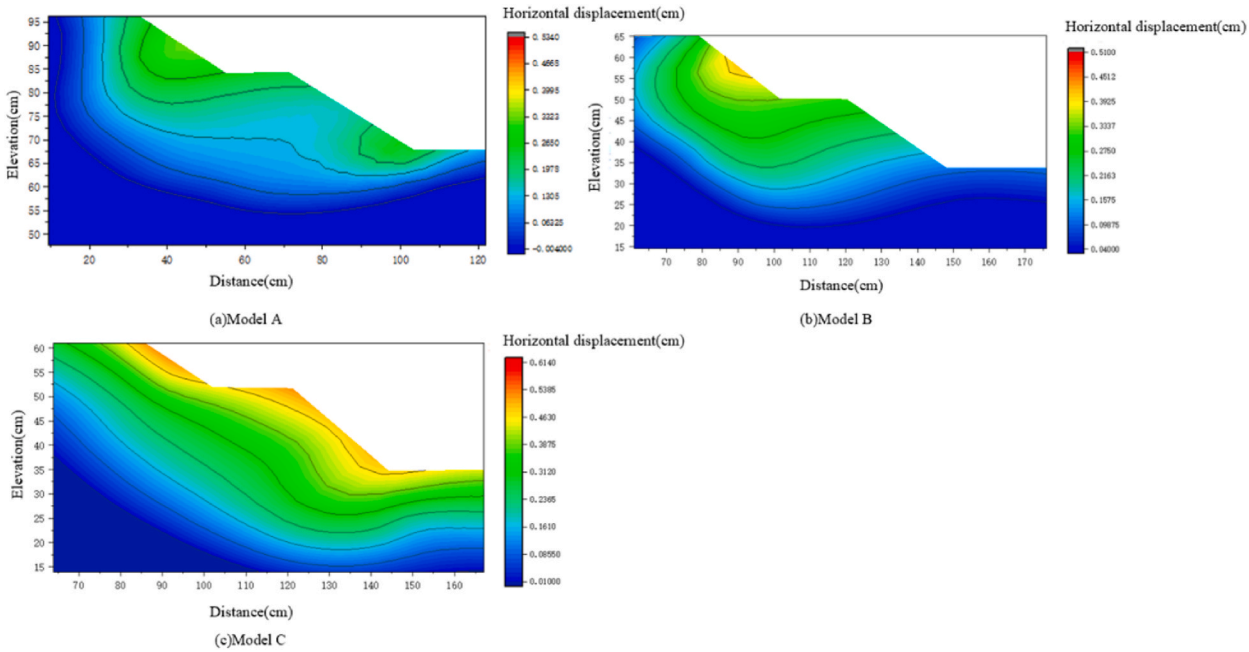

Fig. 11. Horizontal displacement contour maps of models.

between the first bench and the WBS layer, indicating that the sliding mode of Model B successively involves arc-shaped sliding within the dump, linear sliding along the WBS base, and shear cutting along the slope foot of the dump. Compared with Model B, Model C has a further expanded sliding range, and its sliding surface extends from the dump to the loess layer along the WBS layer. The arc-shaped sliding at the first bench is more notable than that at the second bench. The reason is that an increase in thickness of the WBS layer leads to a decrease in overall shear strength in the lower part of the slope. When the upper berm of the second bench gets compressed, cracks are formed within the slope of the second bench, and the WBS layer undergoes shear deformation. As the WBS layer directly contacts the first bench, stress is concentrated on the slope surface of the first bench. When the plastic zones are connected internally,

the entire slope is destroyed. The maximum value of horizontal displacement for the three models grows gradually, and the overall horizontal displacement of the slope also increases unevenly. This phenomenon is explained as follows: the lower shear strength and higher fluidity of WBS relative to loess make it more prone to shear deformation under stress. Moreover, as time goes by, uneven settlement of WBS causes uneven stress on the dump slope. As a consequence, stress can be easily concentrated at the slope of the bench, triggering greater horizontal displacement.

5. Numerical simulation verification

The CAD drawings of the three models were imported into the rhino software for 3D modeling, and then the models were divided into grids with a mesh size of 1 m by griddle plugin (Fig. 12). With the aid of the strength reduction method, the three groups of divided mesh models were imported into the finite difference software FLAC^{3D} for calculation until they converged, and the calculation results are shown in Figs. 13–15 [24].

Fig. 13 reveals that the shear strain increment distribution for the three models follows an arc-shaped pattern. Specifically, in Model A, a connected shear strain zone exists at the slope foot of the second bench, which marks the formation of cracks at the slope foot of the second bench during the failure process. The overall failure mode of the slope is manifested as arc-shaped sliding from the dump to the interior of the loess layer. Model B exhibits a linear shear strain zone along the base of the WBS layer in the middle part. Additionally, a connected shear strain zone is formed at the upper berms of both the first and the second benches, which is indicative of the generation of nearly vertical cracks during the failure process. The sliding mode includes arc-shaped sliding from the upper waste to the interior of the WBS, linear sliding along the base of the WBS layer, and shear cutting along the slope foot. Similar to Model B, Model C also has a connected shear strain zone at the upper berms of both the first and the second benches. Oblique cracks are formed at the upper berm of the first bench and the lower part of the upper berm of the second bench during the sliding process, demonstrating that the sliding mode of Model C is arc-shaped sliding from the dump to the interior of the WBS. As illustrated in Fig. 14, the horizontal displacement distribution for all the models follows an arc-shaped pattern, with the maximum values occurring at the slope angle of the first bench and gradually decreasing inward. Moreover, as the WBS thickens, the overall horizontal displacement variation slows down, which is a mark of transition from sliding to “sliding-settling”. As displayed in Fig. 15, the vertical displacement at the upper berm of the second bench is negative for all the models, indicating settlement at this position. Meanwhile, the vertical displacement at the slope angle of the first bench is larger and in the upward direction, which suggests that the emergence of a “bulging” phenomenon at this position. As Model C has a thicker WBS layer, after the slope is damaged and cracks are formed, the lower berm of the first bench experiences larger settlement due to the uneven tension caused by the settlement of the WBS layer, and the slope foot of the first bench undergoes “bulging” due to compression.

6. Stability calculation of WBS base dump

The safety factor, which refers to the ratio of sliding resistance to sliding force along the assumed sliding surface, is a crucial index for the dump slope stability. When its value exceeds 1, the slope is stable. When its value is below 1, the slope fails. When it equals 1, the slope is in a limit equilibrium state. The relationship between the safety factor of the slope and the thickness of the WBS layer was analyzed by establishing a mechanical model based on limit equilibrium. The sliding surface of the WBS base dump slope is circular. From left to right, the sliding body is numbered from 1 to n by the strip division method, and the i-th soil strip is selected for force analysis (see Fig. 16).

According to the Mohr-Coulomb strength theory, the relationship between the sliding resistance and the safety factor in the limit equilibrium state is:

$$F_{Ti} = \frac{c_i l_i \left(1 - \frac{h_i}{H_i}\right) + F'_{Ni} \tan \phi'_i}{K_s}$$

where F_{Ti} is the sliding resistance of the i-th soil strip; c_i is the cohesion of the waste in the i-th soil strip; h_i is the average thickness of WBS in the soil strip; H_i is the average total thickness of the soil strip; l_i is the arc length of the sliding surface; F'_{Ni} is an effective reverse mana; ϕ'_i is the effective internal friction angle of the i-th soil strip; and K_s is the safety factor.

The soil strip satisfies the stress balance and the torque balance of the sliding body towards the circle center O. The side wall forces of adjacent soil strips are of the same value but opposite directions. Therefore, the torque on Point O can be offset. Considering the above conditions, the safety factor of the slope can be calculated by:

$$K_s = \frac{\sum_1^n \frac{1}{m_i} \left[c_i b_i \left(1 - \frac{h_i}{H_i}\right) + (F_{wi} - u_i b_i) \tan \phi'_i \right]}{\sum_1^n F_{wi} \sin \theta_i}$$

where $m_i = \cos \theta_i + \frac{\tan \phi'_i}{K_s} \sin \theta_i$; b_i is the width of the i-th soil strip; F_{wi} is the weight of the i-th soil strip; u_i is the pore water pressure; and θ_i is the circle center angle of the i-th soil strip.

The relevant parameters were put into the formula for calculation in combination of the actual conditions. In addition, the dump

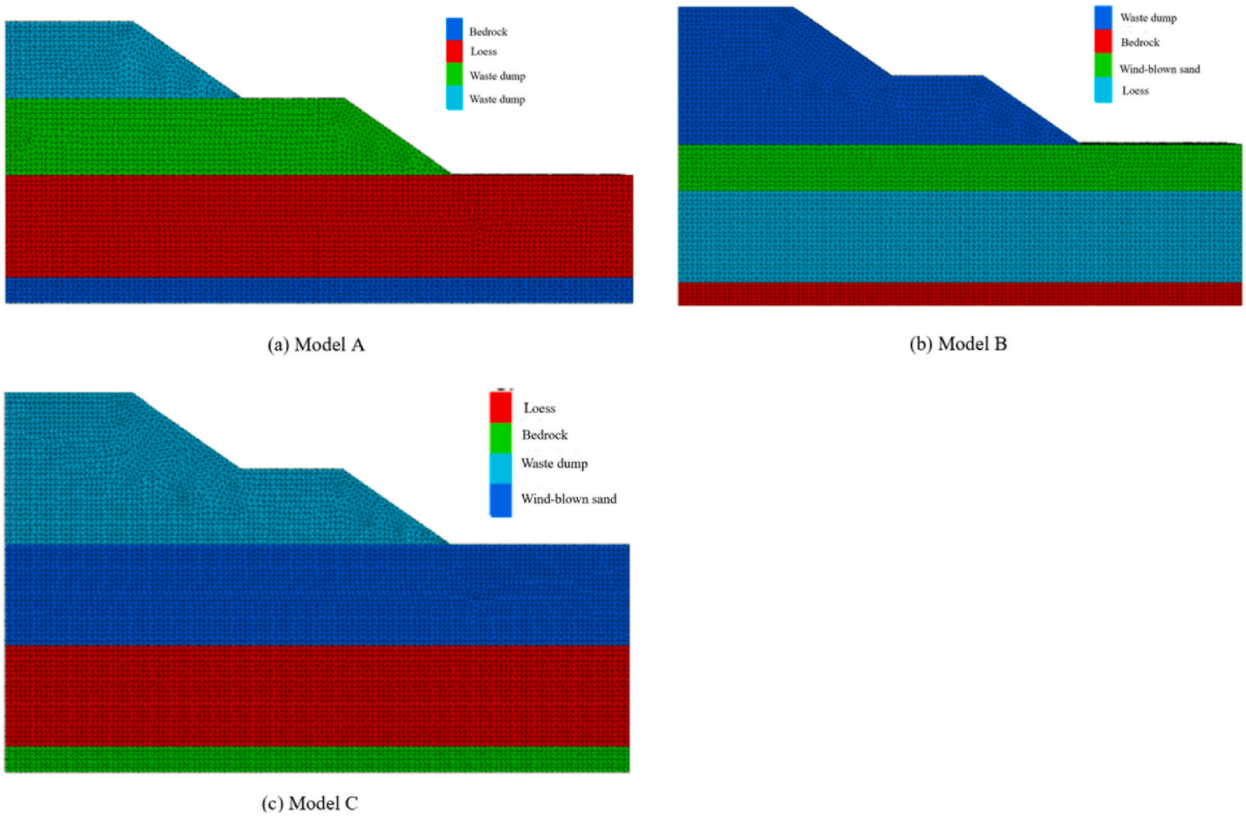

Fig. 12. Grid division of models.

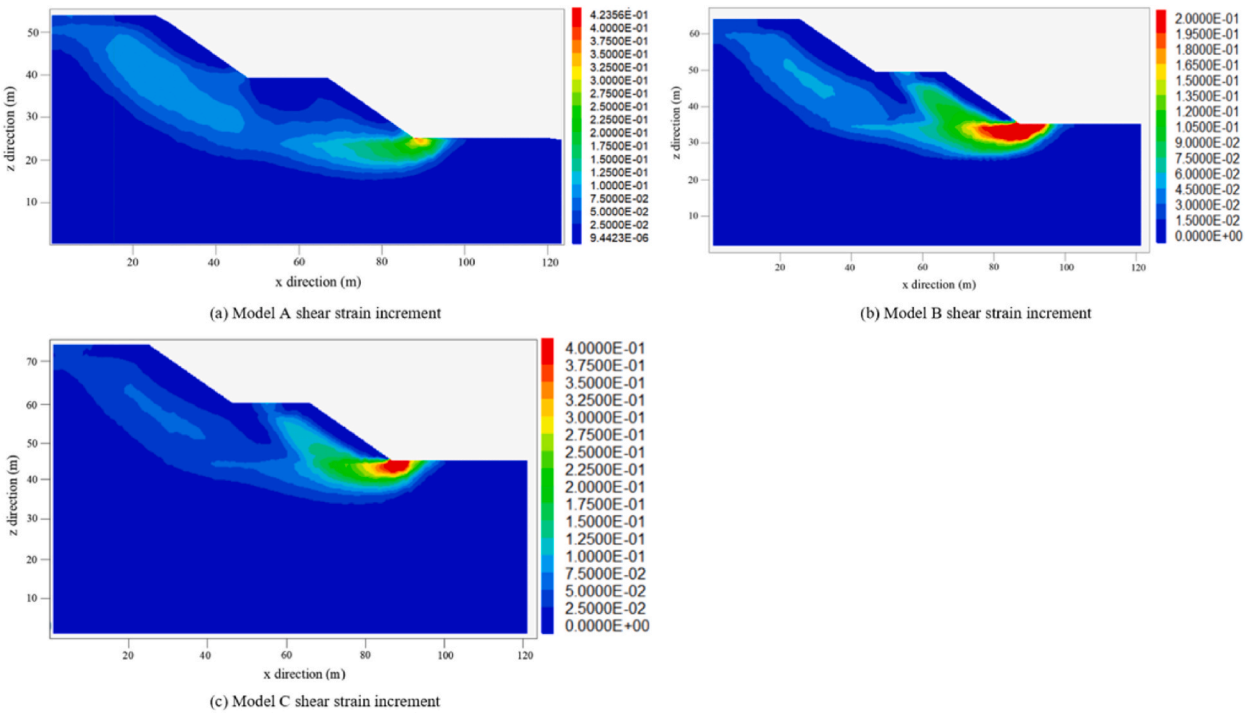

Fig. 13. Comparison of shear strain increment of models.

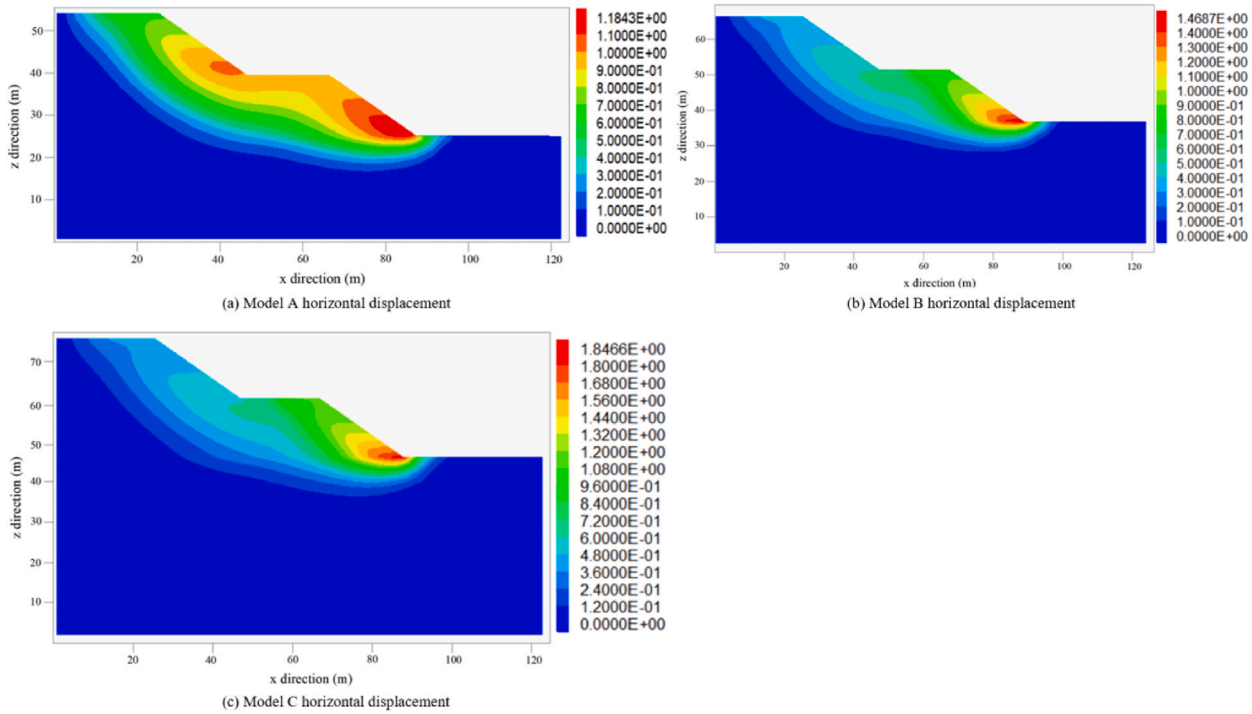

Fig. 14. Comparison of horizontal displacement of models.

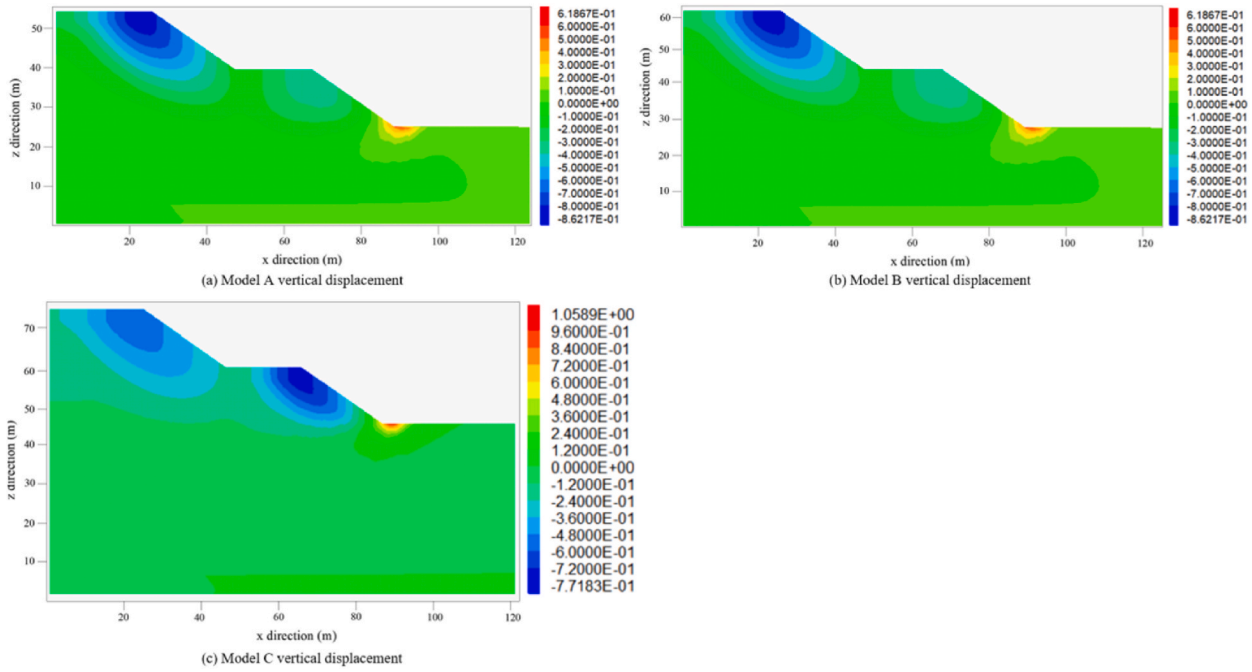

Fig. 15. Comparison of vertical displacement of models.

slope with a WBS layer that was 0–20 m thick was simulated, and its safety factor was calculated by Geo-studio software by the Morgenstern-Price limit equilibrium method. The two groups of data were collated into the curves in Fig. 17.

As presented in Fig. 17, as the WBS layer widens, the safety factor of the slope decreases non-linearly. This is attributed to the following fact. The WBS is extremely loose (cohesion nearly 0), while the waste material corresponds to a far higher cohesion. In this case, when the thickness of the WBS layer starts to increase, the overall shear strength falls quickly, resulting in a plunge of the safety

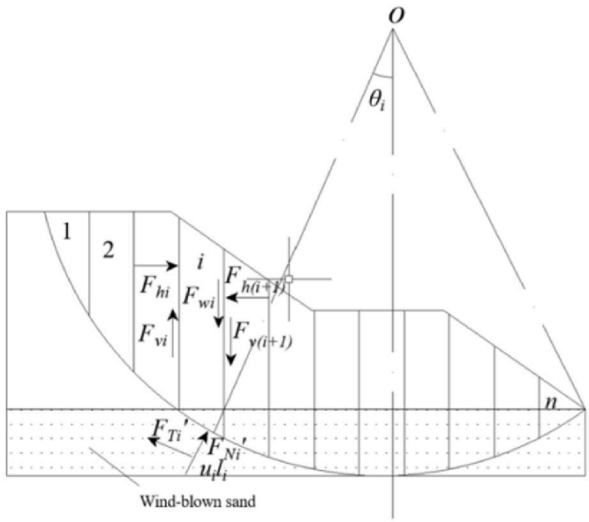

Fig. 16. Soil strip force analysis.

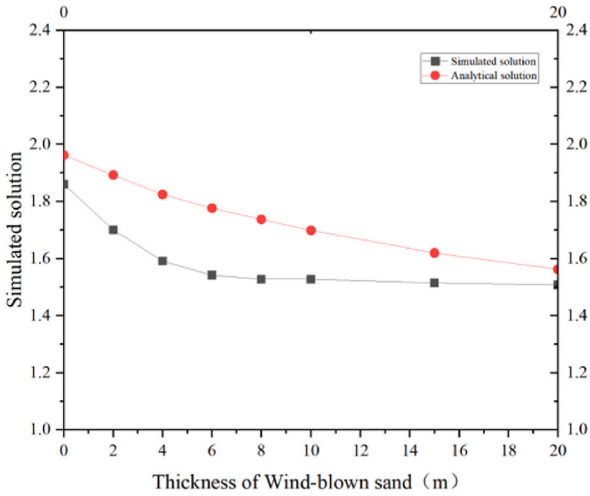

Fig. 17. Relationship between the safety factor of the slope and the thickness of the WBS layer.

factor. However, as the thickness continues to increase, the overall shear strength decreases at a decelerated rate, so that the safety factor decline increasingly slowly.

7. Conclusion

In the light of the principle of similar simulation experiment, three dump slope models with thickness of 0 cm, 10 cm and 20 cm were established, and the three models were successively loaded at the top until they failed. An analysis on the failure of the model unveils that WBS changes the sliding mode of the dump. The original loess-base dump corresponds to internal circular arc sliding, while the circular arc sliding inside the WBS-base dump does not extend to the WBS layer. Instead, it induces linear sliding in the WBS layer and splits at the slope angle. According to the mechanical mechanism, WBS is of strong fluidity, yet low shear strength. When the upper part of the slope is subject to load, the WBS base cannot effectively support the overlying dump, but will be extruded around and settle downward. Moreover, as the WBS layer thickens, the tensile stress caused by the uneven settlement increases, resulting in tensile cracking of the overlying dump and thus generating more cracks than the loess base. Therefore, the stability of the dump slope weakens.

Based on the strength reduction method, the results were verified by the numerical simulation software FLAC^{3D}. From the three aspects of shear strain increment, horizontal displacement, and vertical displacement, the simulated results are basically consistent with the experimental results.

The equation of relationship between the thickness of the WBS layer and the safety factor of the slope was obtained by the limit

equilibrium theory. It is found that the safety factor of the slope decreases non-linearly as the WBS layer thickens. This equation can effectively reflect how the thickness of the WBS layer influences the slope stability. Accordingly, control measures for mining areas with similar geological conditions are put forward: 1) Slope shape should be strictly controlled during soil discharge, and the influence of the thickness of the WBS layer on the slope stability should be considered. A certain margin of margin should be left for the safety factor specified in the regulations. 2) To establish a slope monitoring system, radar monitoring can be used to obtain the displacement of the slope by monitoring slope deformation. Meanwhile, underground monitoring holes can be arranged to grasp the dynamic change law of groundwater in time. 3) Measures can be taken to strengthen the slope at the slope foot. For example, materials can be used to compact the slope foot, or WBS near the slope foot can be compacted to raise its density, so as to improve the stability of the overall dump slope.

Ethics approval and consent to participate

Not applicable.

Data availability statement

All data generated or analyzed during this study are included in this published article.

CRediT authorship contribution statement

Hongze Zhao: Writing – review & editing, Writing – original draft, Project administration, Methodology, Funding acquisition. **Yan Lu:** Writing – original draft. **Binde Qin:** Validation, Formal analysis. **Qiang Hao:** Investigation. **Yu Sun:** Resources.

Declaration of competing interest

The authors declare that they have no known competing financial interests or personal relationships that could have appeared to influence the work reported in this paper.

Acknowledgments

This work was financially supported by the Open Foundation of the State Key Laboratory for Geomechanics and Deep Underground Engineering of China University of Mining and Technology (Beijing) (SKLGDUEK1923), China and the National Key R&D Program (2022YFB4703701), China. Meanwhile, the authors are very grateful for the anonymous reviewers' valuable comments.

References

[1] Li Wenqian, Min Chen, Xiangyu Kou, Stability analysis of open pit dump and landslide prevention measures, Min. Technol. 23 (1) (2023) 59–61.
[2] Ke Rongyong, Application of safety and quality Management in mining, Metall. Manag. (2) (2023) 86–89.
[3] Y. Zerradi, M. Souissi, A. Larabi, Application of the deterministic block theory to the slope stability design of an open-pit mine in Morocco, Min. Miner. Deposits 17 (2) (2023) 53–60.
[4] O. Sdvyzhkova, S. Moldabayev, A. Başçetin, et al., Probabilistic assessment of slope stability at ore mining with steep layers in deep open pits, Min. Miner. Deposits 16 (4) (2022).
[5] S. Sun, Z. Miao, Y. Dong, et al., The slope stability evaluation of open-pit mine based on GIS[C], in: 2015 International Conference on Architectural, Civil and Hydraulics Engineering, Atlantis Press, 2015, pp. 403–408.
[6] Hongzhi Fan, Guangjin Wang, L.A.N. Rong, et al., Study on the influence of weak interlayers on the stability of open-pit rock slope, J. Chongqing Univ. 47 (4) (2019) 22–33.
[7] P.M.V. Nguyen, A. Wrana, S. Rajwa, et al., Slope stability numerical analysis and landslide prevention of coal mine waste dump under the impact of rainfall—a case study of Janina Mine, Poland, Energies 15 (21) (2022) 8311.
[8] Jiachen Wang, Li Yangchun, Xu Wenbin, et al., Failure model and mechanism of soft-steep basement dump slope, J. Min. Sci. 6 (2) (2021) 139–147.
[9] Zhang Yan, Cai Feng, L.I. Haitao, Study on slope failure mode and stability of East open pit dump in Pingshuo, Coal Eng. 52 (9) (2020) 130–134.
[10] Xiangchao Fu, Study on failure mechanism of inner dump in Harusu open-pit Coal Mine, Saf. Coal Mine 48 (6) (2017) 212–214.
[11] Xin Zhang, Zhixiang Yin, Wang Dong, Study on stability of inner dump in Shunxing open-pit with soft basement in-clined, World Sci. Technol. Res. Dev. 37 (2) (2015) 138–140.
[12] O. Igwe, C.N. Ayogu, R.I. Maduka, et al., Slope failures and safety index assessment of waste rock dumps in Nigeria's major mines, Nat. Hazards 115 (2023) 1331–1370.
[13] M. Jayaweera, B. Gunawardana, M. Gunawardana, et al., Management of municipal solid waste open dumps immediately after the collapse: an integrated approach from Meethotamulla open dump, Sri Lanka, Waste Manag. 95 (2019) 227–240.
[14] Li Nailu, Qiaomei Yi, Heng Zhang, et al., Aeolian sand and loess mixed solid packing material physical and mechanical properties research, J. Coal Technol. 40 (5) (2021) 20–24, 10.13301/j.carol carroll nki. Ct. 2021.05.006.
[15] Z.L. Jia, S.W. Yan, Z.L. Huo, Laboratory tests on engineering properties of wind-blown sand, Appl. Mech. Mater. 170 (2012) 706–709.
[16] Shuai Wang, Wenhua Yue, Yiqiang Kang, et al., Wind-blown sand filling mining application status and material performance study, J. Min. Sci. 9 (2) (2024) 217–232, 10.19606/j.carol carroll nki JMST. 2024.02.009.
[17] Chong Chen, Failure Mode and Stability Analysis of Weak Base Dump Slope [D], China University of Mining and Technology, Beijing, 2018.
[18] Zhao Hongze, Qin Binde, Zechen Lin, et al., Similar simulation experiment design of waste dump based on multifunction model box, Exp. Technol. Manag. 40 (3) (2023) 106–112.
[19] Zhao Hongze, Du Hairui, Wang Dongyu, et al. An Experimental Device and Method for Studying Water-Bearing slope[P], CN:110108853,2021-6-25.
[20] Zhanping Bai, Lanzhu Cao, Runcai Bai, Orthogonal experimental study on the ratio of similar materials, Open Pit Coal Min. Technol. (3) (1996) 22–23.

[21] Zhao Bingchao, Yunxiang Ma, Yaxin Guo, et al., Experimental study on mechanical properties of collapsible loess similar materials, Min. Saf. Environ. Protect. 49 (3) (2022) 9–14.
[22] Lei Zhang, Jie Lu, Research and analysis of mining subsidence under loess cover, Coal Min. 23 (4) (2018) 58–61.
[23] Teng Ruixue, Zhao Lichun, Li Wei, Stability analysis and engineering treatment of sand basement dump, Open Pit Min. Technol. 37 (5) (2022) 96–98.
[24] Xinggang Wu, Research on slope support technology of an open pit Mine based on FLAC3D, Resour. Inf. Eng. 37 (6) (2002) 65–68.